

Electron soliton in semiconductor nanostructures

S. Bednarek, B. Szafran,* and K. Lis

Faculty of Physics and Applied Computer Science, AGH University of Science and Technology, al. Mickiewicza 30, 30-059 Kraków, Poland

(Received 5 April 2005; revised manuscript received 8 June 2005; published 5 August 2005)

An electron wave packet formed in a semiconductor heterostructure containing a quantum well covered by a metal surface is considered. It is demonstrated that the potential of the charge induced by the electron wave packet on the conducting surface possesses a component of lateral confinement stabilizing its shape. The existence of electron solitons, i.e., running electron wave packets propagating without changing their shape, is demonstrated. In the scattering phenomena, the electron interacting with the induced charge tends to behave like a classical particle with the backscattering probability approaching a step dependence on the incident momentum as the distance from the metal surface is decreased. This effect enhances the ballistic character of transport for fast electrons and facilitates the trapping of slowly moving electrons.

DOI: [10.1103/PhysRevB.72.075319](https://doi.org/10.1103/PhysRevB.72.075319)

PACS number(s): 73.63.Hs, 05.45.Yv, 05.60.Gg

In nonlinear media, in which the nonlinearity compensates for the dispersion, solitary waves (solitons), i.e., wave packets propagating without changing their shape, can be formed. Such waves are encountered in conducting polymers,¹ in optical fibers,² on the water surface,³ in photorefractive crystals,⁴ and in many other systems. The dispersion is intrinsically present in the kinematics of a free quantum wave packet, formed as a superposition of plane waves (momentum eigenfunctions), leading to spreading of the packet in time. In this paper we show that the interaction of an electron wave packet with a metal surface introduces the nonlinearity necessary to stabilize its shape. Due to the interaction, the wave packet acquires solitonic properties.

The electric field generated by a classical charge in a proximity of a grounded conducting metal plate redistributes the charge in the conductor, leading to an appearance of an induced surface charge. The induced charge is a source of an additional potential attracting the original charge to the conductor. A similar effect is present also in the quantum problem. Its influence on the energy spectra was addressed in the literature on electrostatic quantum dots,⁵⁻⁹ in which the dot-confined electron system interacts with the metal gates lowering its energy. The problem of the potential induced by an external charge in the two-dimensional electron gas (2DEG) confined in the inversion layer in a metal-insulator semiconductor structure^{10,11} was considered a few decades ago. The observation of single-electron aspects of such phenomena requires very low temperatures and structures fabricated with a monolayer precision so such observations have only been realized relatively recently,¹² opening prospects for realization of the single-electron and spintronic devices. The solitonic behavior of the electron wave packets moving in semiconductor quantum wires covered by metal plates was demonstrated by Yano and Ferry.¹³ In this paper we reconsider the effects related to the induced potential and demonstrate a self-trapping mechanism in which the electron solitons can be formed and travel, even without the additional quantum wire confinement potential.

In this paper we consider a planar nanostructure covered by a homogeneous metal surface instead of locally defined split gates used in electrostatic quantum dots.¹⁴ The consid-

ered structure [sketched in Fig. 1(a)] is formed by layers of metal, insulator or semiconducting blocking layer (for instance AlGaAs), and a semiconducting quantum well (for instance, made of GaAs). If we assume that the metal is a perfect conductor and neglect quantum effects in the conductor, the problem of the potential distribution can be solved by the method of images.

For a thin quantum well, the movement of an electron wave packet can be described in the transverse directions (x, y) , in which the electron is free to move. The packet $\psi(x, y)$ formed in the quantum well will find itself in a field of the induced potential given by

$$V(\mathbf{r}) = \frac{e}{4\pi\epsilon\epsilon_0} \int dx' dy' \frac{\rho(x', y')}{\sqrt{(x-x')^2 + (y-y')^2 + 4d^2}}, \quad (1)$$

where e is the electron charge, d is the distance of the quantum well from the metal plate, ϵ is the dielectric constant of the medium, and $\rho(\mathbf{r})$ is the mirror reflection of the packets electron density $|\psi(x, y)|^2$ [see Fig. 1(a)]. The induced electric field contains not only a component attracting the electron to the metal surface but also a component of the lateral confinement oriented to the center of the image charge distribution placed above the center of mass of the original electron wave packet. Therefore, the parallel component of the force acting on the wave packet due to the induced electric field is oriented exactly to the center of the packet's charge distribution.

In the quantum approach the induced potential is calculated as a response of the perturbed medium (the electron gas near the conductor surface) to the external perturbation. The response of the Fermi sea in the metal to an external point-charge electron was considered in Ref. 15 with the linear response theory in the random-phase approximation. It was found¹⁵ that the response potential becomes indistinguishable from the image charge potential at distances from the metal surface that are much larger than the potential screening length in the metal. The applicability of the image-charge method is therefore well justified in the present problem, in which the electron is separated from the metal by at least 5

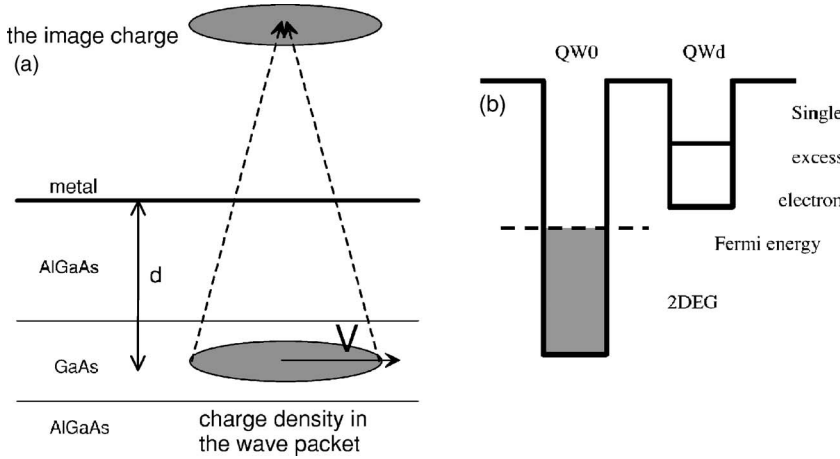


FIG. 1. (a) Schematics of the considered structure, the wave packet, and its image. The solid vector shows the packet velocity, and the dashed vectors indicate the forces acting on the electron in the front and the tail of the wave packet. (b) The model structure used for the discussion of the linear response theory of the induced potential.

nm and the induced potential is also calculated at the same distance. To discuss the response to a diffuse charge, we consider the 2DEG confined in a semiconductor quantum well and its perturbation due to the Coulomb potential of a single electron localized in a nearby, shallower quantum well [see Fig. 1(b)]. Note that the model structure itself can be experimentally realized. We assume that the bottom of the deeper quantum well (QW0) is deep enough below the Fermi level to allow the 2DEG formation, and that the bottom of the shallower well (QWd), containing a single electron, lies above the Fermi level. The wells are separated by the GaAlAs tunnel barrier. We neglect the small variations of the effective mass and dielectric constant in the heterostructure and use the GaAs parameters $m=0.067m_0$ and $\epsilon=12.4$. We assume that the 2DEG is strictly localized at $z=0$ plane and that the single electron in the QWd is localized strictly at $z=d$. Let the single-electron wave function in the transverse direction be given by a Gaussian

$$\psi(\mathbf{r}) = (\pi l^2)^{-1/4} \exp\left(-\frac{x^2 + y^2}{2l^2}\right). \quad (2)$$

The potential V_0^{ext} generated by the electron in QWd is felt by the 2DEG in QW0 as an external potential. The Fourier transform of the potential at $z=0$ is given by

$$V_0^{ext}(\mathbf{k}) = -e\rho_d(\mathbf{k})V^c(\mathbf{k}, d), \quad (3)$$

being a product of the Fourier transform of the electron density in state (2) $\rho_d(\mathbf{k}) = \exp\left(\frac{-k^2 l^2}{4}\right)$ and the Fourier transform of the Coulomb potential (shifted by d in the z direction)

$$\begin{aligned} V^c(\mathbf{k}, d) &= \frac{e}{4\pi\epsilon\epsilon_0} \int dx dy \frac{\exp[i(k_x x + k_y y)]}{\sqrt{x^2 + y^2 + d^2}} \\ &= \frac{e}{4\pi\epsilon\epsilon_0} \frac{2\pi}{k} \exp(-kd). \end{aligned} \quad (4)$$

Linear response of the 2DEG in QW0 on potential (3) yields the induced potential, which in QWd is given by the expres-

$$V_d^{ind}(\mathbf{k}) = \frac{\chi_0(k)[V^c(k, d)]^2 \rho_d(\mathbf{k})}{1 - \chi_0(k)V^c(k, 0)}. \quad (5)$$

We calculate the static density response function of the 2DEG (as in Refs. 10, 11, and 16) obtaining $\chi_0(k) = -me/\pi\hbar^2$, which yields

$$V_d^{ind}(k) = \frac{e}{4\pi\epsilon\epsilon_0} \frac{2\pi}{k} \frac{\exp(-k^2 l^2/4 - kd)}{1 + \epsilon k/4m}. \quad (6)$$

The induced potential in the real space is calculated through an inverse Fourier transform. The comparison of the induced potential calculated by the linear response method and the potential calculated as due to the image charge is given in Fig. 2. The difference between the potentials increases with decreasing spread of the Gaussian, but is small even for the strong localization, which supports the applicability of the image-charge method employed in the present paper. In general, each calculation performed on the ground of the quantum mechanics reducing the many-body problem to the

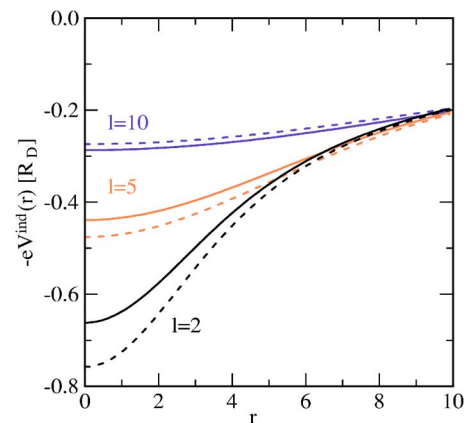


FIG. 2. (Color online) Potential energies in the real space as calculated from the linear response theory (solid lines) calculated for the model sketched in Fig. 1(b) and the potential of the image charge (dashed lines) for various localization lengths l of the electron wave function [cf. Eq. (2)]. Donor Bohr radius $a_D = \hbar^2 \epsilon / me^2 = 9.8$ nm is used as the length unit and the donor Rydberg $R_D = me^4 / 2\hbar^2 \epsilon^2 = 5.93$ meV as the energy unit, with the distance between the quantum wells $d = a_D$.

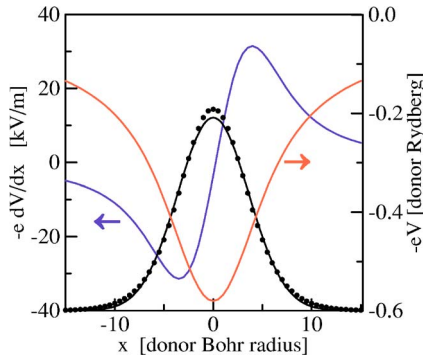


FIG. 3. (Color online) The ground-state eigenfunction of Hamiltonian (7) (dots) and its Gaussian approximation (solid black line) for quantum well-conductor distance d equal to GaAs donor Bohr radius for $y=0$. The red line shows the potential energy of an electron in the induced potential (1) and the blue line, the x component of the induced electric field.

single-electron approximation must inevitably produce an induced potential as a response to the electron-density distribution, i.e., to the square of the modulus of the wave function.

Due to its interaction with the conductor, the electron wave packet becomes self-trapped. The shape of the stable wave packet can be determined by a solution of an eigenequation of the Hamiltonian for an electron in the field of the induced potential

$$H = -\frac{\hbar^2}{2m} \left(\frac{\partial^2}{\partial x^2} + \frac{\partial^2}{\partial y^2} \right) - eV(\mathbf{r}). \quad (7)$$

Since the induced potential (1) depends on the eigenfunction of the Hamiltonian (7) the calculations are performed self-consistently. The wave function of the self-trapped electron has a shape very close to Gaussian. Figure 3 presents a comparison of the stable packet wave function with its Gaussian approximation at d equal to GaAs donor Bohr radius $a_D = 9.8$ nm. The self-trapping potential and the parallel component of the electric field for which the self-consistency is reached are plotted in Fig. 3 with red and blue lines, respectively.

The value of l parameter for which the packet is stable depends on the quantum well-conductor distance d . It turns out that the radius of the stable wave packet is comparable to d and depends on it nearly linearly. In Fig. 4 we also present the dependence of the eigenvalue of Hamiltonian (7) on d (dashed line). Note that the eigenvalue of Eq. (7) is not equal to the total energy of the system. Instead, it has the same interpretation as the single-electron energy in the mean-field calculations. The total energy of the system is obtained by subtracting half of the interaction energy from the eigenvalue (similar to the mean-field calculations); see dotted line in Fig. 4.

The solution of the time-dependent Schrödinger equation for the stable wave packet Ψ_s taken as an initial condition is simply $\Psi(\mathbf{r}, t) = \Psi_s(\mathbf{r}) \exp(-iEt/\hbar)$ [E is the eigenvalue of Hamiltonian (7)] and corresponds to a stationary electron density [see Fig. 5(a)]. For comparison, the solution of the

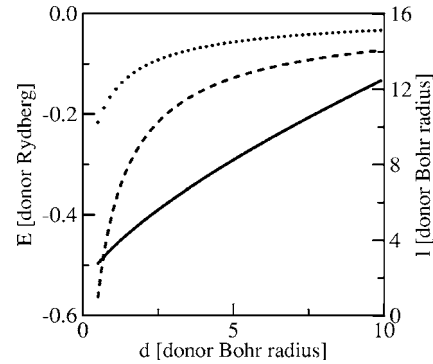


FIG. 4. The radius of the stable wave packet l (solid line, right scale) as a function of the quantum well to conductor distance d . The ground-state eigenvalue of Hamiltonian (7) is plotted with a dashed line and the total energy with a dotted line, both referred to the left axis.

time-dependent Schrödinger equation for the same initial condition but with neglected image-charge effect is shown in Fig. 5(b). In Fig. 5(c) the account¹⁷ is taken for the interaction but the initial condition is set as a Gaussian with the value of the l parameter decreased by 10% from $3.61a_D$ (optimal fit value for $d=a_D$; see Fig. 3) to $3.21a_D$. The wave packet is not stationary, but the self-trapping mechanism prevents it from spreading.

Let us now consider a propagating wave packet. The stationary wave packet is set in motion for the initial condition taken as the stable wave packet Ψ_s multiplied by a plane wave

$$\Psi(\mathbf{r}, 0) = \Psi_s(\mathbf{r}) \exp(ikx). \quad (8)$$

The wave packet moving parallel to the metal surface with a certain low velocity is accompanied by a moving induced

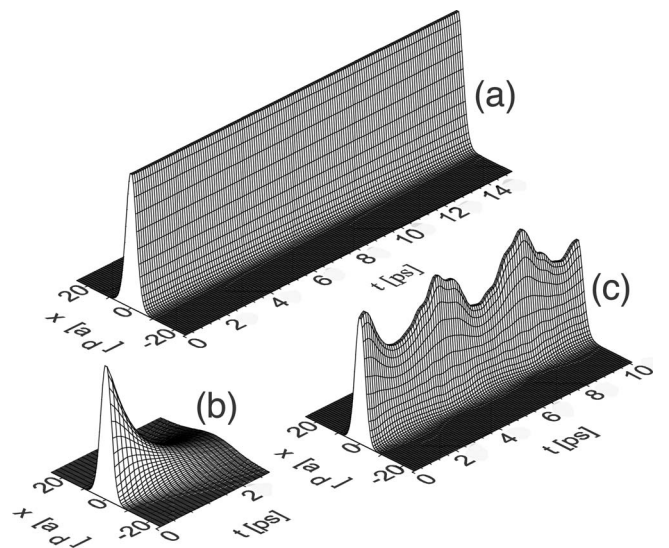


FIG. 5. Electron densities given by the time-dependent Schrödinger equation for $d=a_D$ at $y=0$. The stable wave packet was taken as the initial condition [Eq. (8)] for (a) and (b). In (a) the interaction of the image was accounted for and in (b) it was neglected. Plot (c) shows the time dependence of the electron density for a Gaussian wave packet with $l=3.21$ [see Eq. (3)], i.e., decreased by 10% from the optimal fit to the stable wave packet.

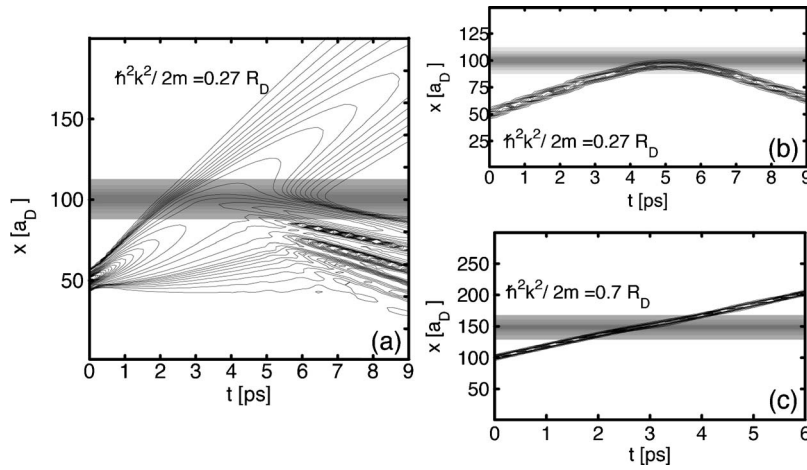


FIG. 6. Time evolution of the electron wave packet moving along a quantum wire and scattering on the potential barrier of a charged acceptor placed at a distance of $5a_d$ from the wire. Contours show the electron wave packet and the shape of the acceptor potential barrier is marked by shades of gray. In (a) and (b) the kinetic energy of progressive movement $\hbar^2 k^2 / 2m$ is set to 0.27 and in (c) to $0.7 R_D$. In (b) and (c) the metallic plate-wire distance is $d=a_d$, and in (a) the metal plate, it is absent.

charge (moving image). For a perfect conductor the redistribution of the induced charge is fast and nondissipative. Note that the force acting on the front of the wave packet has an antiparallel (retarding) component to the wave-packet velocity [cf. Figs. 1(a) and 3] and that the force on the tail of the wave packet has a parallel (accelerating) component to the velocity of the packet. The forces acting on the front and the tail of the wave packet prevent it from spreading when it moves. We have found by numerical simulations for the initial condition (8) that the charge density of the packet moving along the x axis with velocity $V=\hbar k/m$ is unchanged in time. Actually, it can be shown that the stationary and running solitons are related via the Lorentz transformation in the nonrelativistic limit. It is found that the wave function evolves in time according to

$$\Psi(\mathbf{r}, t) = \Psi_s(x - Vt, y) \exp\left(ikx - \frac{i\left(E + \frac{mV^2}{2}\right)t}{\hbar}\right). \quad (9)$$

The self-focusing mechanism has a crucial influence on the scattering properties of a moving electron. We considered an electron confined in a wire placed underneath a metal plate. The electron tunnels through a barrier formed by a distant Coulomb defect of a charged acceptor placed at a distance of $w=5a_d$ from the wire (the maximum of the potential of the impurity $1/\sqrt{x^2+w^2}$ is equal to $0.4R_D$). We assume a negligible width of the wire, reducing the problem to strictly one dimensional and neglect the image charge of the acceptor. For the initial condition we took the electron eigenstate calculated in the absence of the Coulomb defect for $d=a_d$ multiplied by a plane wave [Eq. (8)]. Figures 6(a) and 6(b) show the results for the kinetic energy of the progressive movement of $k^2/2m=0.27R_D$ for an electron noninteracting (a) and interacting (b) with the metal plate. A larger part of the free wave packet [Fig. 6(a)] is reflected, but in the soliton packet of Fig. 6(b) the tunneling through the impurity potential barrier is totally suppressed. On the other hand, for higher k , the entire soliton packet is transferred through the barrier [see Fig. 6(c) for $\hbar^2 k^2 / 2m = 0.7R_D$]. The transfer probability is plotted in function of the kinetic energy in Fig. 7 for $d=a_d$, $2a_d$ and ∞ (free wave packet). We notice that with the decreasing wire-metal plate distance the dependence becomes more stepwise. In the scattering phenomena, the

electron interacting with the induced charge tends to behave like a classical particle. This effect can essentially facilitate the electron control in the single-electron devices. In the presence of a metal plate, slowly moving electrons will be trapped more easily in local potential cavities and the transport of electrons traveling with larger velocities will have more ballistic character. The presented effect of the induced-charge-assisted ballistic transport indicates that the experimental verification of the solitonic electron behavior can be performed in the conductance measurements.

Due to a relatively small binding energy the soliton can possibly be observed only in low temperatures. For a GaAs/AlGaAs nanostructure the soliton binding energy at $d=20$ nm is about -0.1 meV. The soliton will be destroyed by thermal excitations above 1 K. Nevertheless, in temperatures in which the electrostatic quantum dots are studied,¹⁴ the soliton effect should be observable. More favorable conditions for the soliton observation are expected to be found in structures based on semiconductors with larger effective masses and smaller dielectric constants.

We have shown that an electron in a semiconductor nanostructure under a metal surface can travel in form of a wave

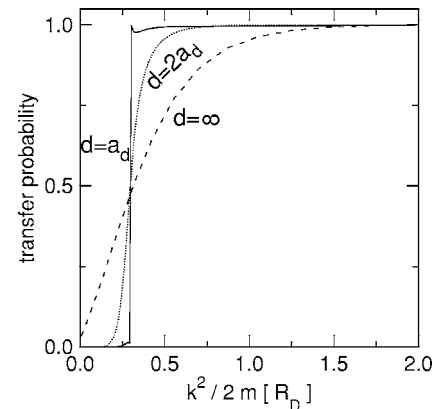


FIG. 7. Transfer probability as function of the kinetic energy of the incident electron wave packet for the potential barrier of a distance-charged acceptor (see Fig. 5). Solid, dotted, and dashed curves correspond to the metal surface at $d=a_d$, $2a_d$, and ∞ , respectively.

packet of a stable shape having all the characteristics of a soliton. Formation of solitons can essentially change the low-temperature behavior of carriers close to electrodes deposited on the nanostructure. In particular this effect will influence the transport and scattering properties of the carriers, their capacity of passing through obstacles (tunneling through barriers and potential wells) affecting the effective resistance.

The self-trapping mechanism should facilitate the control of carriers in single-electron devices, which can be useful for designing the quantum gates as well as in spintronic applications.

This paper was supported by the Polish Government for Scientific Research (KBN) under Grant No. 1P03B 002 27.

*Present address: Departement Fysica, Universiteit Antwerpen, Groenenborgerlaan 171, B-2020 Antwerpen, Belgium.

¹A. J. Heeger, S. Kivelson, J. R. Schrieffer, and W.-P. Su, *Rev. Mod. Phys.* **60**, 781 (1988).

²H. A. Haus and W. S. Wong, *Rev. Mod. Phys.* **68**, 423 (1996).

³A. R. Osborne, E. Segre, G. Boffetta, and L. Caveri, *Phys. Rev. Lett.* **67**, 592 (1991).

⁴J. W. Fleischer, T. Carmon, M. Segev, N. K. Efremidis, and D. N. Christodoulides, *Phys. Rev. Lett.* **90**, 023902 (2003).

⁵P. Hawrylak, *Phys. Rev. Lett.* **71**, 3347 (1993).

⁶N. A. Bruce and P. A. Maksym, *Phys. Rev. B* **61**, 4718 (2000).

⁷S. Bednarek, B. Szafran, and J. Adamowski, *Phys. Rev. B* **61**, 4461 (2000).

⁸S. Bednarek, B. Szafran, and J. Adamowski, *Phys. Rev. B* **64**, 195303 (2001).

⁹S. Bednarek, B. Szafran, K. Lis, and J. Adamowski, *Phys. Rev. B* **68**, 155333 (2003).

¹⁰F. Stern, *Phys. Rev. Lett.* **18**, 546 (1967).

¹¹T. Ando, A. B. Fowler, and F. Stern, *Rev. Mod. Phys.* **54**, 437 (1982).

¹²R. C. Ashoori, H. L. Stormer, J. S. Weiner, L. N. Pfeiffer, S. J. Pearton, K. W. Baldwin, and K. W. West, *Phys. Rev. Lett.* **68**, 3088 (1992).

¹³K. Yano and D. K. Ferry, *Superlattices Microstruct.* **11**, 61 (1991).

¹⁴J. M. Elzerman, R. Hanson, L. H. Willems, L. M. K. Vandersypen, and L. P. Kouwenhoven, *Appl. Phys. Lett.* **84**, 4617 (2004).

¹⁵D. E. Beck and V. Celli, *Phys. Rev. B* **2**, 2955 (1970).

¹⁶E. Zaremba, I. Nagy, and P. M. Echenique, *Phys. Rev. B* **71**, 125323 (2005).

¹⁷In the time-dependent calculations we neglect the time delay in the redistribution of the induced charge, i.e., the image charge in each timestep is set identical to the original electron distribution.